Ecología Austral 35:193-209 Agosto 2025
Asociación Argentina de Ecología
https://doi.org/10.25260/EA.25.35.2.0.2475

Climate change in North Patagonian Andes: Recent temperature and precipitation trends

Nicolás Martyniuk

Laboratorio de Limnología, INIBIOMA, CONICET-UN del Comahue. Bariloche, Argentina.

Abstract. This study examines climate change in the North Patagonian Andes (NPA), analyzing temperature and precipitation trends over the last three decades. Using data from 12 key meteorological stations, we assessed changes in mean annual temperatures and precipitation patterns, with a focus on lee-side precipitation suppression across two 100 km West-East transects: the La Angostura (40.75° S) and Manso (41.5° S) transects. Results reveal a consistent warming trend across all stations, most pronounced at Alerce station in the NPA, where temperatures increased by 0.82 °C per decade since 1993. This warming intensified after 2007, marked by rising temperature anomalies and more frequent hot extremes. Precipitation trends show significant declines in both transects, as reflected in the standardized precipitation index, with moderate to severe droughts becoming increasingly common since 2016. Precipitation trends revealed a notable decline since 2007, especially in the Manso transect, which was more affected by the westward retraction of precipitation isohyets in the last 5 years (2016-2021). These patterns are likely associated with the positive phase of the Southern Annular Mode (SAM), which has driven poleward shifts in storm tracks, reducing NPA precipitation. The observed climate changes have critical implications for regional hydrology and ecosystem dynamics, highlighting the need to monitor interactions between atmospheric circulation (e.g., SAM) and local climate variability. Our findings underscore the urgency of understanding these processes to anticipate impacts of ongoing climate change in the NPA.

[Keywords: temperature anomaly, SPI, latitudinal transect, Manso, SAM, positive phase]

Resumen. Cambio climático en los Andes Norpatagónicos: Tendencias recientes de temperatura y precipitación. Este estudio examina el cambio climático en los Andes Norpatagónicos (NPA), analizando las tendencias de temperatura y precipitación durante las últimas tres décadas. Utilizando datos de 12 estaciones meteorológicas clave, evaluamos los cambios en las temperaturas medias anuales y los patrones de precipitación, con un enfoque en la supresión de precipitación en la ladera de sotavento a lo largo de dos transectas oeste-este, de 100 km: las transectas La Angostura (40.75° S) y Manso (41.5° S). Los resultados revelan una tendencia de calentamiento consistente en todas las estaciones, más pronunciada en la estación Alerce dentro del NPA, donde las temperaturas aumentaron 0.82 °C por década desde 1993. Este calentamiento se intensificó después de 2007, marcado por el aumento de anomalías térmicas y eventos cálidos extremos más frecuentes. Las tendencias de precipitación muestran disminuciones significativas en ambas transectas, reflejadas en el índice estandarizado de precipitación, con sequías moderadas a severas cada vez más comunes desde 2016. Se observó un declive notable en la precipitación desde 2007; en especial, en la transecta Manso, más afectada por el retroceso hacia el oeste de las isoyetas de precipitación en los últimos 5 años (2016-2021). Estos patrones probablemente están asociados a la fase positiva del Modo Anular del Sur (SAM, por sus siglas en inglés), que ha impulsado un desplazamiento hacia el polo de las trayectorias de tormentas, reduciendo la precipitación en el NPA. Los cambios climáticos observados tienen implicaciones críticas para la hidrología regional y para la dinámica de los ecosistemas, y destacan la necesidad de monitorear las interacciones entre la circulación atmosférica (e.g., SAM) y la variabilidad climática local. Nuestros hallazgos subrayan la urgencia de comprender estos procesos para anticipar los impactos del cambio climático en curso en el NPA.

[Palabras clave: anomalía de temperatura, ISP, transecta latitudinal, Manso, MAS, fase positiva]

Editora asociada: Rosina Soler
✉ nmartyniuk@comahue-conicet.gob.ar

Recibido: 13 de Octubre de 2024
Aceptado: 29 de Marzo de 2025

Introducción

The recent increase in greenhouse gases in the atmosphere has caused global mean temperatures to rise to levels previously seen in geological time. However, the rate of this increase has never been seen before (Marcott et al. 2013; IPCC 2021). The average temperature of the Earth's surface has increased during the last 125 years. Still, this increase has not been uniform across the planet due to changes in regional topography, mountain ranges, the climatic effect of the oceans and other factors (IPCC 2021). The upward trend in globally averaged temperatures suggests that more regions are experiencing warming than cooling. According to NOAA's 2021 Annual Climate Report (Lindsey and Dahlman 2020), land and ocean temperatures have increased at an average rate of 0.08 °C per decade since 1880. However, the average rate of increase since 1981 has been more than twice as fast, with an increase of approximately 1.5 °C in land and ocean temperature since 1880. Thus, each of the last four decades has been successively warmer than any decade that preceded it since 1850 (IPCC 2021).

When the temperature changes, it directly affects the amount, strength, frequency and type of precipitation (Giorgi et al. 2019). For instance, even a slight increase of 0.5 °C in global warming can lead to noticeable gains in the strength and frequency of hot weather and heavy rainfall, according to the Intergovernmental Panel on Climate Change - IPCC (2021). The warming of the air can also speed up the drying of soil and make droughts more severe, which has been observed in many regions, including South America, as reported by Rivera and Penalba (2014) and Morales et al. (2020). In addition, precipitation quality could also change, as temperatures rise, and the likelihood of precipitation falling as rain rather than snow increases (Huss et al. 2017; Cordero et al. 2019). Such changes are observed in many places, especially over land in middle and high latitudes in both hemispheres IPCC (2021), leading to increased rains but reduced snowpacks and accumulation in glaciers (Cordero et al. 2019; Condom et al. 2020).

Climate change potentially affects the aquatic environment by changing water quantity and quality (Lauro et al. 2019; Masiokas et al. 2019; IPCC 2021). The impacts can vary between catchments depending on local climate and catchment characteristics, which are specific to each watershed process. Hydrological systems that originate in mountainous regions are more vulnerable to climate-induced changes, leading to greater fluctuations in water quantity (Huss et al. 2017; Pessacg et al. 2020). North Patagonian Andes (NPA) located in the mid-latitudes of South America, contains one of the largest lake districts in the Andes (Messager et al. 2016) and is the source of one of the major headwaters of Patagonian rivers, such as the Limay-Neuquén-Negro River Basin (González 2015; González et al. 2022). This river system drains an area of 140000 km^2 and constitutes the most important hydrographic system of all those that extend entirely into the Argentine territory (González 2015; González et al. 2022). The Andes in this sector are primarily influenced by the westerlies (Paruelo et al. 1998), which exhibit a pluvial regime characterized by peak discharges during the winter primarily due to rainfall, and a secondary peak in spring resulting from snow and ice melt (González 2015). In addition, since the 1950s, there has been a reduction in this basin of the mean annual flow of up to 30% since 2000 (González and Vera 2010). Over the past few decades, consistent variations in precipitation and air temperature in the North Patagonian Andes have become evident through observable changes in aquatic habitats, including lakes, rivers and glaciers (Masiokas et al. 2019; Masiokas et al. 2020; Pessacg et al. 2020).

The interannual climate variability of the NPA is influenced by large-scale modes such as the El Niño-Southern Oscillation (ENSO) and the Southern Annular Mode (SAM) (González and Vera 2010; González et al. 2015; Berri et al. 2019; Campbell and Renwick 2023). ENSO modulates global climate through changes in tropical convection. At the same time, SAM is characterized by a latitudinal oscillation of tropospheric-deep westerly winds over the mid-to-high latitudes of the Southern Hemisphere (Arblaster and Meehl 2006; Campbell and Renwick 2023). In recent decades, the amplitude of ENSO has generally weakened (Berri et al. 2019; Lauro et al. 2019). However, El Niño events still have a noticeable impact between 38° S and 45° S, particularly during the summer months (Arias et al. 2021).

Additionally, greenhouse gas emissions and ozone depletion have driven a significant trend toward the positive phase of SAM (Berri et al. 2019). The poleward migration of the westerly winds associated with the positive phase of SAM has resulted in decreased precipitation

at mid-latitudes of the Andes (Arblaster and Meehl 2006; Fogt and Marshall 2020). The combined effects of ENSO and SAM are projected to further alter temperature and precipitation patterns over the NPA.

The IPCC has divided the world into several regions to ensure consistent climate signals and climatological coherence (IPCC 2021). Although the NPA is in the Southwestern South America (SWS) region, the western limit of the Southern South America (SSA) region is very close to the NPA. Given the proximity of the SSA, which is described as having a predominantly cold desert climate, one of the purposes of this study is to investigate the changes that have occurred in the SWS/SSA border over the past 30 years. Therefore, the study is presented in three main parts. The first part, the interannual analysis of temperature in NPA, aims to identify the shift in temperature trends, anomalies, and the occurrence of hot/cold events, through an analysis of annual time series. The second part aims to highlight the changes in precipitation using seasonal and spatial analyses. Two latitudinal transects were used to examine trends over time (months and rainy season) and distance (from the NPA to the SWS/SSA boundary). Lastly, the third part of the manuscript provides a comprehensive discussion of the results, including their potential linkage with changes in climate drivers such as the ENSO and the SAM and possible environmental impacts. These analyses give baseline information to reduce uncertainty caused by spatial heterogeneity in general circulation and regional climate models for predicting short- and long-term scenarios. Thus, local analyses of temperature and precipitation patterns enhance our understanding of climate change (Condom et al. 2020; Arias et al. 2021).

Materials and Methods

Study area characterization

Located in southern South America (36° S - 45° S), the NPA's climate is primarily shaped by mid-latitude westerlies. Seasonal changes in the Southern Andes are driven by shifts in the westerlies' position and strength, influenced by the southeast Pacific high-pressure system (Paruelo et al. 1998; Fogt and Marshall 2020). Weather disturbances and westerly winds from the Pacific Ocean are more frequent and intense in winter. Additionally, from 38° S to 45° S, El Niño-Southern Oscillation (ENSO)-related precipitation anomalies occur in summer, with Patagonia receiving less precipitation during La Niña years and more during El Niño years (Garreaud 2018; Berri et al. 2019; Arias et al. 2021). The region is also affected by the Southern Annular Mode (SAM), the most significant pattern of atmospheric variability in the Southern Hemisphere's middle and high latitudes. SAM correlates with rainfall, snowfall, and droughts in the southern Andes (Garreaud 2009; Silvestri and Vera 2009). The NPA, therefore, experiences a combination of ENSO and SAM effects.

Due to the North-South alignment of the Andes, perpendicular to prevailing westerlies, there is a marked precipitation gradient across the range. Around 40° S - 41° S, the North Patagonian Andes receives ~3000 mm/y of precipitation, while the central Patagonian steppe receives ~200 mm/y (Jobbágy et al. 1995; Paruelo et al. 1998).

Meteorological data

Meteorological data from 12 weather stations (Table 1) within 40°50′ S - 42° S and 72° W - 70°50′ W were used (Figure 1). The temperature was analyzed at Alerce, Bariloche (BRC) Airport, and El Bolson (Figure 1), the only stations with over 50 years of continuous records in North Patagonia. Annual precipitation was examined along two 100 km west-east transects, La Angostura and Manso, selected for their over 20 years of data and strategic west-east distribution across the North Patagonian Andes. The data from El Bolson, Alerce, Manso Inferior, Steffen, Villegas and Las Bayas stations were obtained from the National Water Information System of the Secretary of Infrastructure and Water Policy of Argentina (SNIH, snih.hidricosargentina.gob.ar). Meteorological data from BRC Airport station were obtained from the Meteorological Information Center of the National Meteorological Service (SMN, smn.gob.ar). All precipitation data for meteorological stations in the La Angostura latitudinal transect were sourced from the Interjurisdictional Basin Authority of the Limay, Neuquen, and Negro Rivers (AIC).

Temperature data collection varied across stations; while some had continuous records (e.g., hourly in BRC Airport), others recorded only three or four measurements per day (e.g., Alerce). To standardize mean temperature records, all stations used the average of three daily measurements (9 a.m., 3 p.m., and 9

Table 1. Details of meteorological stations and data used in the analyses.
Tabla 1. Detalles de las estaciones meteorológicas y de la información utilizada en los análisis.

Site	Location		Altitude (m a. s. l.)	Period		Data source
	Latitude	Longitude		Precipitation	Mean temperature	
BRC Airport	-41.13	-71.13	840	1994-2021	1962-2021	SMN[1]
Alerce	-41.35	-71.72	770	1955-2021	1955-2021	SNIH[2]
El Bolson	-41.98	-71.52	483	1994-2021	1964-2021	SNIH
Manso Inferior	-41.56	-71.78	443	1994-2021	-	SNIH
Steffen	-41.50	-71.54	565	1994-2021	-	SNIH
Villegas	-41.59	-71.49	572	1994-2021	-	SNIH
Las Bayas	-41.51	-71.17	949	1994-2021	-	SNIH
Cerro Mirador	-40.72	-71.93	1261	2001-2021	-	AIC[3]
El Rincón	-40.73	-71.80	777	2001-2021	-	AIC
Villa La Angostura	-40.78	-71.66	769	2001-2021	-	AIC
La Cantera	-40.72	-71.11	709	2001-2021	-	AIC
Corralito	-40.73	-70.69	660	2001-2021	-	AIC

1=Servicio Meteorológico Nacional (smn.gob.ar)
2=Sistema Nacional de Información Hídrica (snih.hidricosargentina.gob.ar)
3=Autoridad Interjurisdiccional de Cuencas (aic.gob.ar)

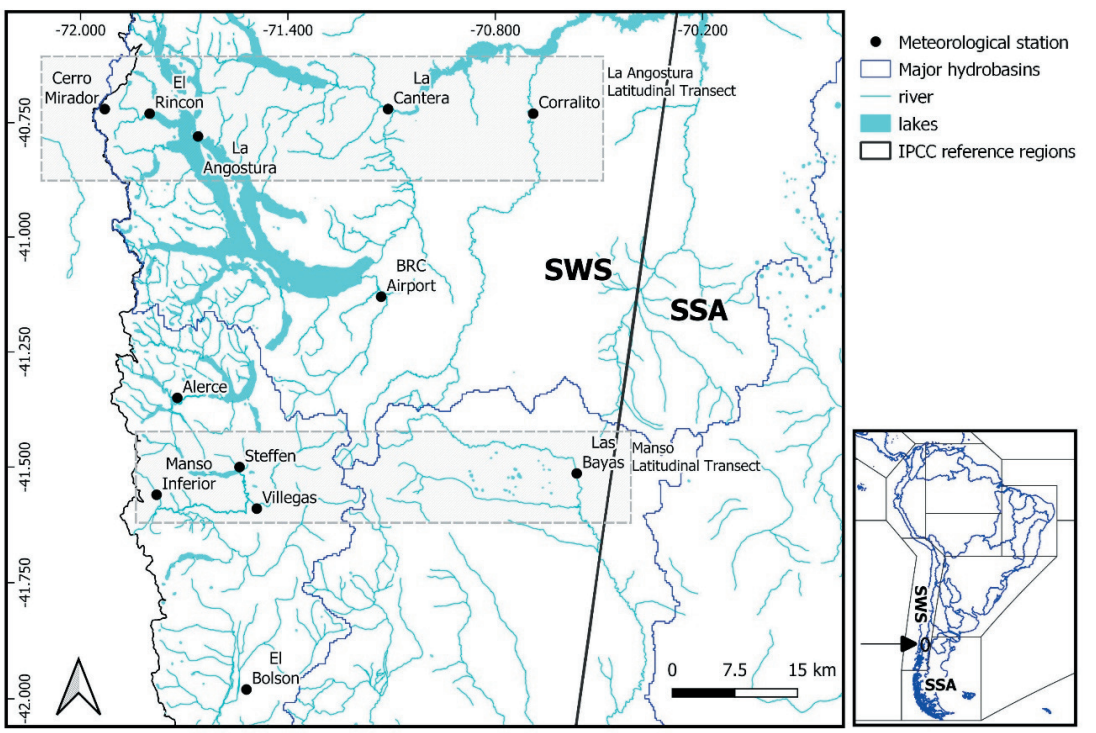

Figure 1. Location of meteorological stations and latitudinal transects. IPCC climatic regions: Southwestern South America (SWS) and Southern South America (SSA).

Figura 1. Ubicación de las estaciones meteorológicas y de las transectas latitudinales. Regiones climaticas del IPCC: Sudoeste de América del Sur (SWS) y Sur de América del Sur (SSA)

p.m.). Before 1994, Alerce had 5% missing data, while BRC Airport and El Bolson had ~1% gaps. Missing values were filled using an adapted version of Fernández et al. (2020), leveraging nearby SNIH and SMN stations to calculate monthly mean differences and standard deviations for data adjustment. The resulting mean difference was used to adjust the data in the auxiliary dataset before filling in the gaps in the primary dataset.

The remaining gaps were filled via linear interpolation (Luedeling 2018). Precipitation data had no missing values.

Temperature analyses

The historical temperature records from BRC Airport, Alerce, and El Bolson were modeled using a seasonal-trend decomposition procedure based on LOcally wEighted Scatterplot Smoothing (LOESS) (Cleveland and Grosse 1991). Seasonal-trend decomposition based on LOESS is a filtering procedure for decomposing a seasonal time series into three components: trend, seasonal and remainder or residual. Since all meteorological stations have their temperature records complete (without filling gaps) from 1994, trend decomposition of daily mean temperature was performed from January 1, 1994, to December 31, 2021.

Annual temperature anomalies were calculated for BRC Airport, Alerce, and El Bolson from the beginning of their temperature records and were analyzed using the 1981-2010 period as the reference. This baseline period is globally used and was defined by the World Meteorological Organization (WMO) (WMO 2021) and IPCC (IPCC 2021). Extreme weather events would normally be as rare as, or rarer than the 10th or 90th percentile of a probability density function estimated from observations (IPCC 2014). Thus, extreme event temperatures less than the 10th percentile (MIN) were classified as cold events, and temperatures higher than the 90th percentile (MAX) were classified as hot events, based on a probability density function estimated from observations. The probability density function was calculated from observations during the reference period 1981-2010. Due to the gaps in minimum and maximum temperature records across all meteorological stations, mean temperatures were used to calculate extreme events. While this is not ideal, it provides an approximation of the frequency/probability of these events. Extreme events were calculated for each meteorological station (BRC Airport, Alerce, and El Bolson) during summer and winter. The frequency of extreme hot and cold events was expressed as the percentage of days with extreme temperatures in each season (90-91 days in summer and 92 days in winter). For instance, if 50% of the mean temperatures are categorized as hot events, it indicates that on 45 days, the mean temperature surpassed the 90th percentile of the average mean temperature for the 1981-2010 period.

Precipitation analyses

Meteorological data from stations located in La Angostura and Manso latitudinal transects were used to detect patterns in annual and monthly precipitation. Both analyses were conducted using generalized additive models (GAM) (Wood 2008). GAM analysis was chosen for its ability to handle non-linear relationships between the response variable and the set of explanatory variables (Guisan et al. 2002). An advantage of GAM over traditional regression techniques is that it does not require an a priori specification of the shape of the relationship between dependent and independent variables (Wood 2008). The amount of non-linearity (i.e., the complexity of the smoothing function) was determined by an automatic cross-validation routine (mgcv package) using R (R Core Team 2020). In all cases, fitted GAMs were estimated using maximum likelihood-based smoothness selection procedures, particularly the restricted maximum likelihood (REML). Model assumptions were checked using residual plots. A spatial interpolation of rainfall patterns in the NPA was performed using Kriging, a Bayesian inference-based geostatistical interpolation technique for estimating values at unmeasured locations (Kleijnen 2017).

Drought conditions were estimated using the standardized precipitation index (SPI) (McKee et al. 1993; Guttman 1999), which compares precipitation over a given period to historical records. While the SPI is not a drought forecasting tool, it has been used to identify dry and wet conditions (Guttman 1999). The further the SPI value deviates from zero, the more unusually dry (negative) or wet (positive) the period is. SPI values were calculated monthly (SPI) and over 6-month periods (SPI-6m), then averaged for each latitudinal transect. The SPI-6m value in September represents the accumulated rainfall from April until September (SPI-9). SPI-9 was used in this study because the rainfall season in the NPA occurs during this period (González 2015; González et al. 2015). SPI values below -1.0 indicate drought, with three severity levels: extremely dry (SPI<-2), severe dry (-2 to -1.5), and moderate dry (-1.5 to -1). Normal conditions correspond to SPI values between -1 and 1, while values above 1 indicate wet conditions. SPI data were generated using the SPI Generator Program (National Drought Mitigation Center 2018).

Results

Temperature trends

Alerce, the westernmost station, exhibited a different trend before the 1990s compared to the other stations. From the mid-1960s to the early 1990s, Alerce's annual, 5-year and 10-year moving average temperatures decreased, unlike BRC Airport and El Bolson, which did not show this trend (Figure 2a). From the early 1990s onward, all three stations followed a similar warming pattern. Alerce had the highest increase in mean temperature from 1990 to 2021, with a total rise of 2.46 °C (0.82 °C per decade), while El Bolson increased by 1.59 °C (0.53 °C per decade) (Figure 2a). BRC Airport showed the smallest rise of 0.30°C, at a rate of 0.10°C per decade (Figure 2b). This trend was further confirmed by daily mean temperatures (Supplementary Material-Figure S1), with synchronized warming observed at all stations from 1994 to 2021, especially after 2007 (Supplementary Material-Figure S1). The warm climate from the early 1990s to 2021 was reflected in the annual temperature anomalies (reference period 1981-2010) (Table 1, Figure 2a). Anomalies were consistently positive since 2007 at Alerce (0.2 °C to 2.73 °C), from 2011 at El Bolson (0.5 °C to 1.80 °C) and at BRC Airport (0.3 °C to 1.30 °C) (Figure 2b). Western stations showed higher anomalies,

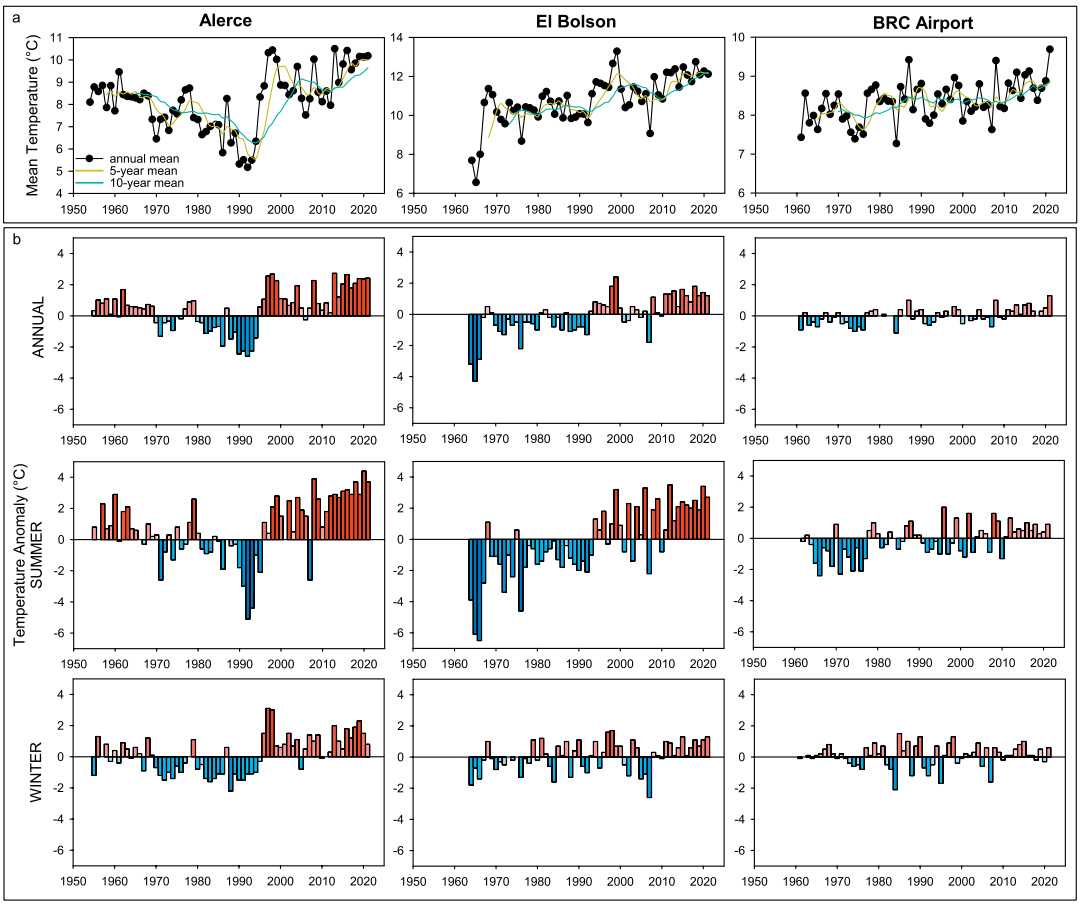

Figure 2. a) Comparison of annual temperature variation among Alerce, Bolson and BRC Airport stations. Solid lines showed the variability of mean temperature with a periodicity of 5 years (red) and 10 years (blue). b) Comparison of temperature anomalies among Alerce, Bolson and BRC Airport stations, and among seasons: winter (June to August) and summer (December to February). The estimated anomalies were derived from data collected between 1981 and 2010 at each station. An alternating blue-red scale was used to depict temperature anomalies, with dark blue <-4 °C and dark red >2 °C.

Figura 2. a) Comparación de la temperatura media anual entre las estaciones de Alerce, Bolsón y el Aeropuerto BRC. Las líneas muestran la variabilidad de la temperatura con una periodicidad de 5 años (rojo) y 10 años (línea azul). b) Comparación de las anomalías de temperatura entre las estaciones de Alerce, Bolsón y el Aeropuerto BRC, y entre estaciones: invierno (de junio a agosto) y verano (de diciembre a febrero). La anomalías fueron estimadas a partir de las temperaturas en el periodo 1981 y 2010. Se utilizó una escala que alterna azul-rojo para distinguir las anomalías de temperatura, siendo el azul oscuro <-4 °C y el rojo oscuro >2 °C.

Table 2. Temperatures of reference for extreme event classification according to the IPCC. Extreme events were temperatures below 10% (MIN) or above 90% (MAX). The reference period was 1981-2010.

Tabla 2. Las temperaturas de referencia para la clasificación de eventos extremos según el IPCC. Los eventos extremos se clasifican como aquellos con temperaturas por debajo del percentil 10% (MIN) o por encima del percentil 90% (MAX).

		Reference mean temperature (°C)	Extreme weather event limit (°C)		Temperature extreme events range (Cold-Hot)
	Site	(1981-2010)	Cold	Hot	
Annual	Alerce	7.9	1.9	15.1	13.2
	Bolson	10.9	3.5	18.9	15.4
	BRC Airport	8.4	1.3	15.9	14.6
Summer	Alerce	13.0	7.9	18.3	10.4
	Bolson	17.4	12.5	22.5	10
	BRC Airport	14.5	10.1	18.7	8.6
Winter	Alerce	3	0.1	6.1	6
	Bolson	4.6	0.9	8.3	7.4
	BRC Airport	2.7	-1.3	6.3	7.6

particularly in summer and winter, while the eastern station experienced colder winter anomalies (Figure 2b).

From daily temperatures (Table 2), a clear shift occurred around 2010, when hot events began to outnumber cold events in both

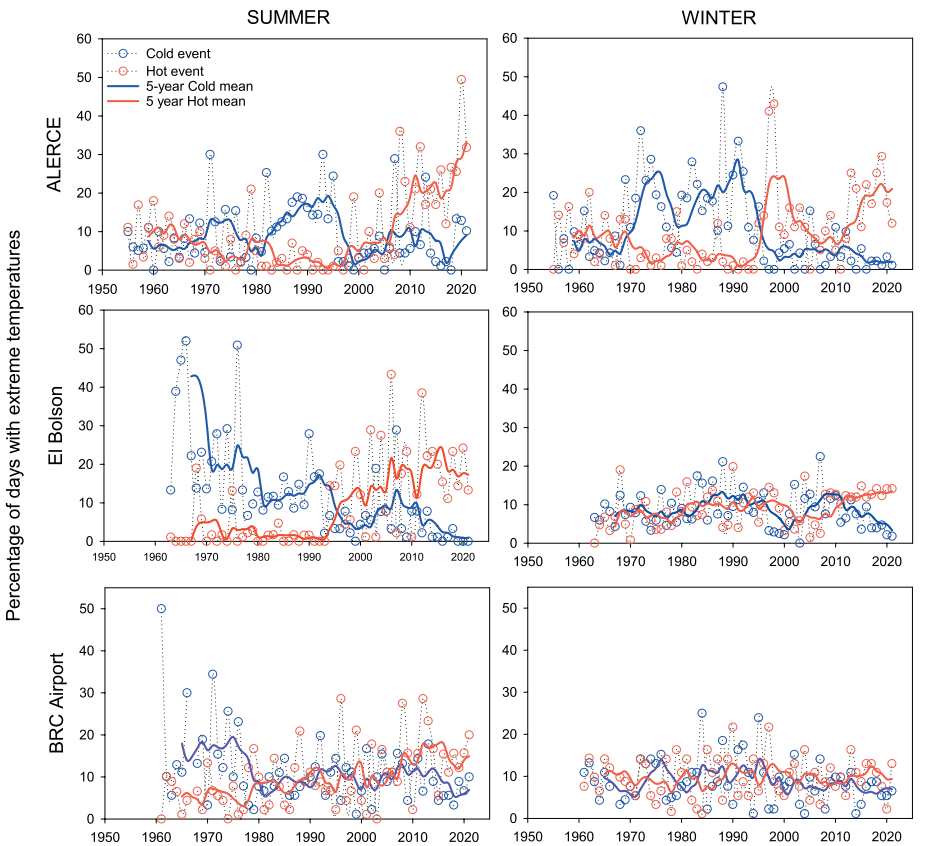

Figure 3. Comparison of extreme weather events (hot and cold) based on mean temperatures among Alerce, Bolson and BRC Airport stations between winter (June to September) and summer (December to March). Solid lines with a 5-year moving average showed a trend in the frequency of extreme heat and cold events (red or blue solid line). Extreme weather events were estimated based on Table 2 reference values. Refer to the Materials and Methods section for calculation information. The percentage of days with extreme temperatures was determined using the time-lapse of each season (summer: 90-91 days, winter: 92 days).

Figura 3. Comparación de eventos meteorológicos extremos (calor y frío) basados en las temperaturas medias entre las estaciones de Alerce, El Bolsón y BRC Airport durante el invierno (de junio a septiembre) y el verano (de diciembre a marzo). Las líneas sólidas con un promedio móvil de 5 años muestran la tendencia en la frecuencia de eventos de calor y frío extremos (línea roja o azul). Los eventos extremos se estimaron según los valores de referencia de la Tabla 2. Consultar la sección Materials and Methods para información sobre el cálculo. El porcentaje de días con temperaturas extremas se determinó según la duración de cada estación (verano: 90-91 días, invierno: 92 días).

summer and winter at all stations (Figure 3). Alerce recorded a rise in hot events post-1990s, replacing earlier cold events (Figure 2b). In summer, cold events were more frequent from 1970-1990, then decreased sharply, with hot events rising from 5% in 2000 to ~40% by 2020-2021 (Figure 3). At El Bolson, summer cold events dropped from ~50% in 1960 to <5% in 2021, while hot events increased from the mid-1990s (Figure 3). Winter events at El Bolson showed no clear pattern until after 2010 when hot events became more common. BRC Airport exhibited a milder trend, with cold events in summer ranging from 10% to 50% between 1960 and 1980, before slightly increasing hot events. Since 2010, cold events have dropped to around 5%, with hot events in summer remaining above 10%, peaking at 25%. Winter temperatures at BRC Airport remained relatively stable, with no clear trends in cold or hot events (Figure 3). Since 2010, hot events have become more frequent than cold events. Temperature anomalies show that hot events were more frequent in the western NPA.

Precipitation: spatial and temporal trends

Precipitation varied notably across the study region. Western stations (i.e., Cerro Mirador, Rincón, Villa La Angostura and Manso Inferior) received more rainfall than eastern ones, with northern stations (Figure 4a, Table 3) also wetter than southern ones (Figure 4b, Table 3). From 2001 to 2021, Rincón received 1596 mm more annual precipitation than Manso Inferior, despite their similar longitudes. In contrast, eastern stations showed smaller differences. For example, Las Bayas and Corralito had comparable mean annual precipitation (230.29 vs. 279.14 mm/y), though Corralito was generally wetter.

Interannual variability was lower in western/northern stations than in southern ones. Cerro Mirador, Rincón and La Angostura had the lowest variability (CV=15.42%, 18.7% and 17%, respectively), while Las Bayas had the highest variability (81%) (Table 3). This high variability likely affected the lack of significance in the long-term downward precipitation trend at the eastern station (Figures 4a,b). However, the eastern stations of La Cantera and Corralito, along with all stations of the Manso transect (Supplementary Material-Table S1, Figure 5a,b) exhibited a significant decline in June precipitation. July precipitation also decreased at most Manso stations (except Las Bayas) (Supplementary Material-Table S1, Figure 5b). As a result, annual precipitation dropped by 50-70% over 20 years in La Cantera, Corralito and Las Bayas, compared to a 10-30% decline in western stations (Figure 4a,b). Despite regional differences, the western stations (i.e., Cerro Mirador, Rincón, Manso Inferior, Steffen and Villegas) showed a significant long-term negative precipitation trend (Supplementary Material-Table S2, Figure 4).

The overall trend masks higher interannual variability in western stations, where more extreme values occurred outside the 95% confidence interval (e.g., Rincón, Cerro Mirador, La Angostura, Manso Inferior, Villegas and Steffen) (Figure 4a,b). Some stations recorded up to 10 extreme years, including Manso Inferior (18 years), Steffen (12), Cerro Mirador (12), Villegas (11) and Rincón (10). Conversely, eastern stations had fewer extreme precipitation values but higher CV (%) due to the greater interannual precipitation variability (Table 3). For instance, La Angostura had only 4 extreme values; Las Bayas, 6; La Cantera, just 1; and Corralito, none (Figure 4a,b). To analyze spatial precipitation shifts, additional stations (Alerce, El Bolson, BRC Airport) were included (Figure 6). Over the past 20 years, higher precipitation isohyets

Table 3. Summary of statistical parameters of the precipitation calculated for each meteorological station over the specified period: annual and April to September (SPI-9).

Tabla 3. Resumen de los parámetros estadísticos de la precipitación calculados para cada estación meteorológica durante un período especifico: anual y de abril a septiembre (SPI-9).

	Annual precipitation		April - September precipitation			
Site	Mean	CV (%)	Mean	CV (%)	% of annual precipitation	Period
Cerro Mirador	4034.0	15.4	2721.3	14.4	67.74	2001-2021
El Rincón	2934.5	18.7	2037.1	16.2	70.06	2001-2021
Villa La Angostura	1566.3	17.0	1147.4	16.8	73.63	2001-2021
La Cantera	898.8	22.7	707.1	27.9	78.36	2001-2021
Corralito	279.1	35.6	224.0	38.6	79.77	2001-2021
Manso Inferior	1424.9	42.1	1006.0	44.3	70.23	1993-2021
Steffen	1064.1	42.5	745.1	43.1	69.92	1993-2021
Villegas	614.1	61.4	440.7	67.6	68.80	1993-2021
Las Bayas	215.8	80.8	167.9	88.9	73.57	1993-2021

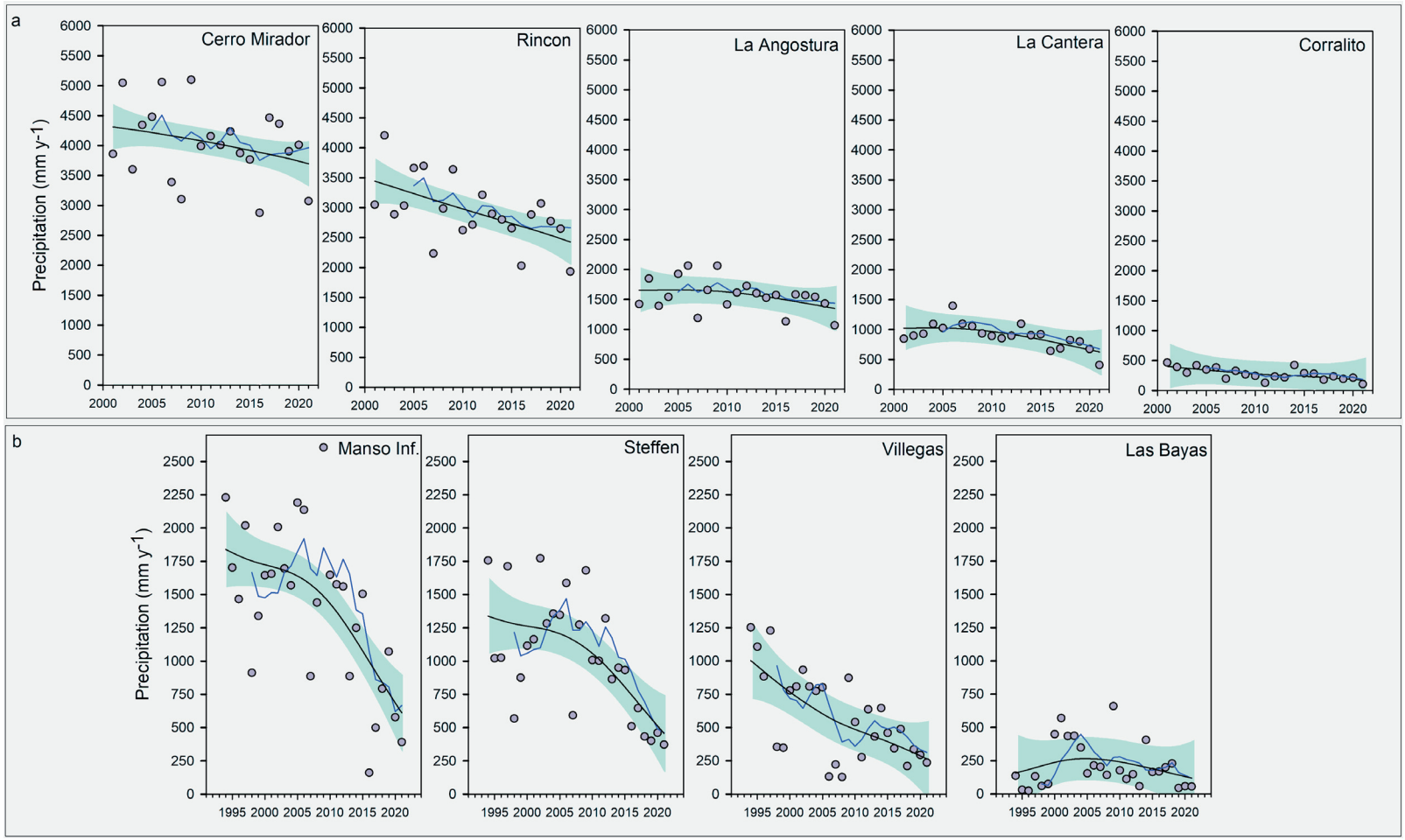

Figure 4. a) Annual precipitation in La Angostura. b) Annual precipitation in Manso latitudinal transect. GAM fit and 95% (interval of confidence) are shown on each station, for GAM fit details see Supplementary Material. Solid lines with a 5-year moving average showed a trend in annual precipitation.

Figura 4. a) Precipitación anual en La Angostura. b) Precipitación anual en la transecta latitudinal del Manso. Se muestran el ajuste GAM y el 95% (intervalo de confianza) en cada estación; para detalles del ajuste GAM, consultar el Material Suplementario. Las líneas sólidas con un promedio móvil de 5 años mostraron una tendencia en la precipitación anual. Líneas de colores representan la tendencia de una media móvil de 5 años en la precipitación anual.

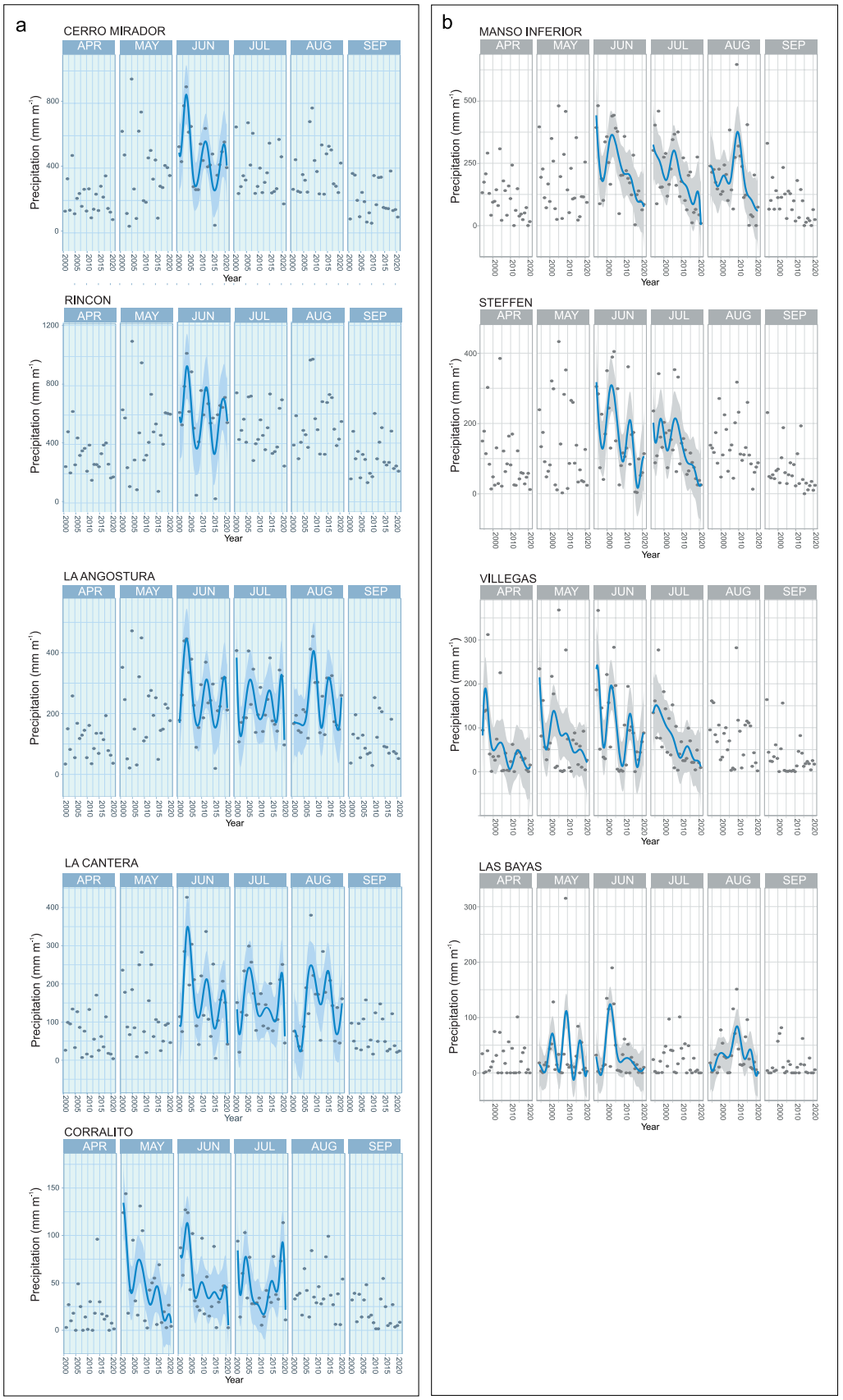
a
CERRO MIRADOR
RINCON
LA ANGOSTURA
LA CANTERA
CORRALITO
b
MANSO INFERIOR
STEFFEN
VILLEGAS
LAS BAYAS
APR
MAY
JUN
JUL
AUG
SEP
Precipitation (mm m-1)
Year

Figure 5. a) Monthly (April to September) precipitation trend analysis at La Angostura Transect stations from 2001 to 2021. b) Monthly precipitation trend analysis at Manso Transect stations from 1994 to 2021. Only significant monthly GAM trends (year: month, P<0.05) with a 95% confidence interval (shadow area) are shown. Supplementary Material-Table S1 contains GAM details.

Figura 5. a) Análisis de la tendencia de la precipitación mensual (de abril a septiembre) en las estaciones de la transecta La Angostura desde 2001 hasta 2021. b) Análisis de la tendencia de la precipitación mensual en las estaciones de la transecta Manso desde 1994 hasta 2021. Se muestran solo las tendencias mensuales significativas (año: mes, P<0.05) del GAM con un intervalo de confianza del 95% (área sombreada). Ver Material Suplementario-Tabla S1 para detalles del GAM.

retracted westward, while lower precipitation isohyets (e.g., 500 and 250 mm) expanded eastward (Figure 6). While western regions consistently received more rainfall, the 2016-2021 period showed a distinct northwest-southeast gradient.

The SPI (Figure 7) confirmed declining interannual precipitation, with a more pronounced trend in the Manso transect (Figure 7b) than in La Angostura (Figure 7a). In La Angostura, SPI 6-m became more negative after 2016, indicating moderate dryness (-1) by 2021. Manso showed a steady decline since 2010, remaining near -1 after 2016. Normal conditions (SPI between -1 and 1) were most frequent, but moderate/severe droughts became more common after 2016,

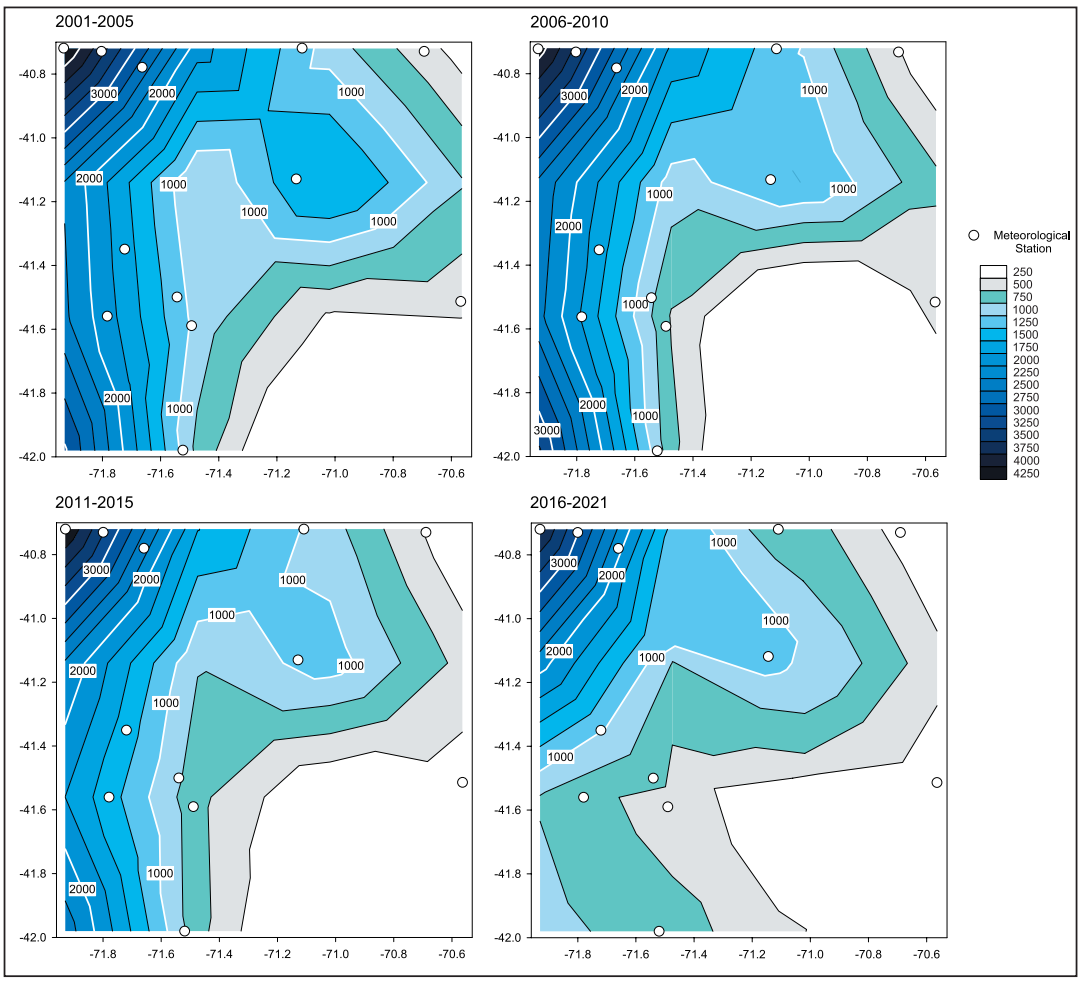

Figure 6. Isohyets are based on a 5-year precipitation average for the period 2001-2021. The white circle represents the meteorological stations along the La Angostura and Manso latitudinal transects and those at Alerce, Bolson and BRC Airport (see references in Figure 1). The contour interval is 250 mm/y, with white lines highlighting multiples of 1000 mm/y.

Figura 6. Las isohietas se muestran como el promedio de precipitación cada 5 años para el período 2001-2021. El círculo blanco representa las estaciones meteorológicas a lo largo de las transectas latitudinales de La Angostura y Manso, así como las estaciones en Alerce, Bolsón y el Aeropuerto BRC (ver Figura 1 para referencia). El intervalo de contorno es de 250 mm/año, las líneas blancas destacan los múltiplos de 1000 mm/año.

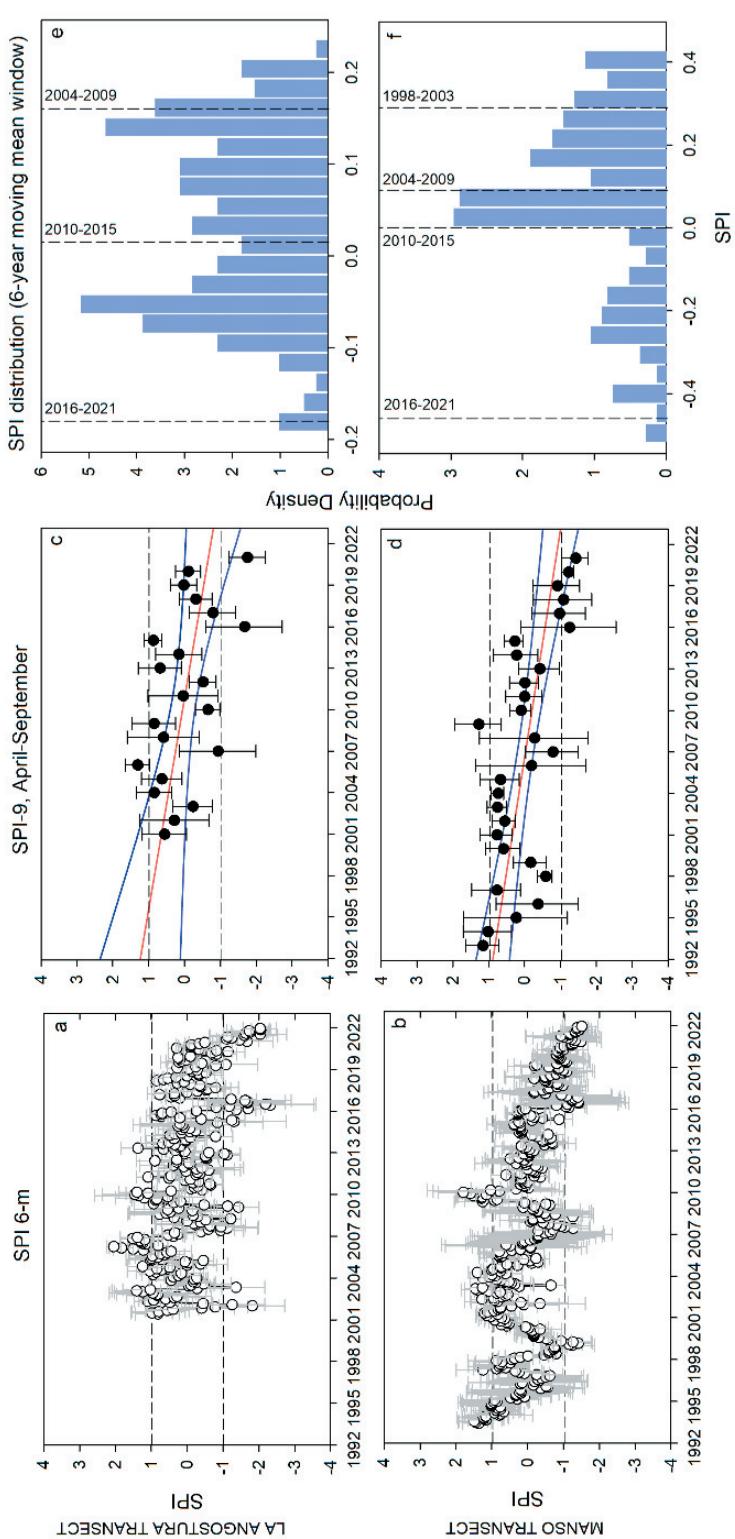

Figure 7. a) and b) Evolution of six-month-standardized precipitation index (SPI 6-m). c) and d) During the rainy season (SPI-9, April-September) in La Angostura and Manso latitudinal transects. e) and f) SPI values distribution with a 6-year moving mean window and average SPI value for the last 3 and 4 6-year periods (dashed lines) in La Angostura and Manso latitudinal transects. SPI 6-m was presented as the mean of all stations along each latitudinal transect and year and the corresponding standard deviation (SD). Linear regression was used to analyze each latitudinal transect's mean (±SD) of the 6-month standardized precipitation index in September (SPI-9, April-September). The red solid line represents a linear regression trend, and the blue line represents the 95% confidence interval. Table 3 provides statistics about April-September precipitation (SPI-9).

Figura 7. a) y b) Evolución del índice estandarizado de precipitación a seis meses (SPI-6). c) y d) Durante la temporada de lluvias (SPI-9, abril-septiembre) en las transectas latitudinales de La Angostura y Manso. e) and f) Distribución del SPI con una ventana móvil de media de 6 años y valor promedio del SPI para los últimos 3 y 4 períodos de 6 años (líneas discontinuas) en las transectas latitudinales de La Angostura y Manso. El SPI-6 se presentó como el promedio de todas las estaciones a lo largo de cada transecta latitudinal y año, así como la desviación estándar (DS) correspondiente. Se utilizó una regresión lineal para analizar el promedio (±DS) de cada transecta latitudinal del índice estandarizado de precipitación a seis meses en septiembre (SPI-9, abril-septiembre). La línea roja continua representa la tendencia de regresión lineal, y la línea azul muestra el intervalo de confianza del 95%. La Tabla 3 proporciona información estadística sobre la precipitación abril-septiembre (SPI-9).

particularly in Manso. The rainy season SPI (SPI-9) also showed significant negative trends in both transects (Figure 7c,d), with similar slopes (-0.061±0.013 in Manso, and -0.065±0.027 in La Angostura). From 2010 to 2015, both remained near the mean (SPI=0), but 2016-2021 was the driest period (Figure 7e,f). This shift was more severe in Manso (-0.46) than in La Angostura (-0.18) latitudinal transect. Notably, since 2016, La Angostura's rainy season briefly recovered (-2 to 0, except in 2021) (Figure 7c), while Manso remained near -1 (Figure 7d). Over the last 18 years in La Angostura and 24 years in Manso, conditions have progressively shifted from wet to dry (Figure 7e,f).

Discussion

North Patagonian Andes revealed significant trends in temperature and precipitation analyses over the past decades. Data from three key stations (BRC Airport, Alerce, and El Bolson) showed a consistent warming trend from 1994 to 2021. This warming trend was further emphasized by a steeper increase in the mean temperature trend starting in 2007, along with a rise in temperature anomalies and more frequent hot weather events since 2010. Additionally, precipitation trends have become more negative, particularly in the Manso transect, which is more affected by the westward retraction of precipitation isohyets. The standardized precipitation index (SPI 6-month and SPI 9-month) also revealed a drought process over the past 18 years in the Manso and La Angostura latitudinal transects, with moderate and severe droughts becoming more frequent since 2016.

Temperature trends

A clear warming trend was observed across the NPA, with significant spatial variability. Western stations in mountainous areas (Alerce and El Bolsón) exhibited pronounced warming since the 1990s, exceeding +0.5 °C per decade. In contrast, BRC Airport —the easternmost station— recorded a markedly smaller temperature increase (~0.3 °C total from 1990-2021), representing a rate five to eight times lower than western sites. This spatial contrast aligns with broader regional patterns: between 1979 and 2006, the Andes of central and northern Chile (17° S - 37° S) warmed at +0.25 °C per decade, while coastal stations experienced cooling (−0.2 °C per decade) (Falvey and Garreaud 2009). Elevation-dependent warming (Vuille et al. 2015) explains BRC Airport's muted trend. Yet post-2007, all stations warmed synchronously —a shift tied to the SAM's positive phase, which raises mid-latitude pressure (40° S - 50 °S)—, weakening polar influences and enhancing warming (Garreaud 2009; Fogt and Marshall 2020).

In the last 40 years, NPA drastically transitioned from common cold events and negative temperature anomalies (1980 to mid-1990) to hot and positive temperature anomalies (from mid-1990). Like what was observed in the mean temperature analyses, western stations (Alerce and El Bolson) were more affected by the warming signal. Thus, in Alerce station since 2007 every year has exhibited a warm anomaly (from +0.2 to +2.37 °C) and a higher occurrence (around 20-30%) of hot weather events in both summer and winter. According to (Fogt and Marshall 2020) from 2008 to 2021, 65% of months exhibited positive SAM values, compared to 55% (1994-2007), 48% (1980-1993) and 41% (1966-1979). This change in SAM could have influenced the steeper mean temperature trend since 2007 and increased the frequency of warm events, but this needs to be tested. Other studies in southern South America have observed that temperature extremes increased more for warm extremes than for cold extremes (Rusticucci and Barrucand 2004; Olmo et al. 2020).

Precipitation: spatial and temporal trends

A mid-1990s study in southern NPA (42° S - 43.5° S) found a west-east precipitation gradient, with eastern areas receiving ~80% less rain (Jobbágy et al. 1995). Now, 30 years later, the gradient in central NPA (40.75° S - 42° S) is even steeper, with eastern stations receiving 7-14 times less precipitation. As observed by Jobbágy et al. (1995), western stations in both transects showed low interannual variability. In contrast, eastern stations exhibited greater variability (i.e., Las Bayas: CV=80%) and a steeper decline in annual precipitation, ~50-70% over the past 20 years. Meanwhile, western stations experienced a more moderate reduction (10-30%). The Manso transect displayed higher variability (CV=42-81%) and a more pronounced precipitation decline compared to La Angostura (CV=15-35%). Overall, northern and western stations showed the least change, whereas southern and eastern stations —located farther from the NPA range— experienced the sharpest declines.

Recent evidence suggests that positive SAM index values are likely unprecedented in the last millennium (Fogt and Marshall 2020) and may be driving a poleward shift in storm tracks (Campbell and Renwick 2023). The low-pressure systems migrate southward, altering mid-latitude precipitation patterns (Fogt and Marshall 2020), especially in winter (Berman et al. 2012; Hurtado et al. 2023). As observed, precipitation peaks occur during autumn-winter (April-September), contributing between 68% and 80% of the annual total. This suggests that changes in low-pressure positioning could strongly influence annual precipitation. Precipitation in June has declined at eastern La Angostura and all Manso stations, while the western Manso stations also experienced a decrease in July. The observed decline aligns with storm track migration (Berman et al. 2012; Arias et al. 2021; Campbell and Renwick 2023). While higher precipitation isohyets have retracted westward and narrowed over the past 20 years, low precipitation isohyets have expanded in area, particularly those in the 750-1000 mm/y range. The sharpest declines and isohyet shifts since 2016 likely signal an advance of the SWS/SSA boundary toward the NPA.

In South America, the 2016 megadrought has been extensively studied, with both a strong El Niño event (akin to the 1997-1998 event) and a persistent positive SAM phase identified as primary contributors to one of the most severe droughts on record (Garreaud 2018; Arias et al. 2021). However, in the years following this event, the Manso transect remained in severe drought (SPI around -1), while the La Angostura transect recovered to mean conditions (near the SPI mean, SPI=0). This difference may be attributed to the northern NPA being less affected by the positive phase of the SAM and instead experiencing wetter conditions driven by other teleconnections, such as ENSO, influenced by El Niño and La Niña events. Nevertheless, the Manso and La Angostura transects have experienced prolonged drought —18 and 24 years, respectively— with the past six years being the driest in the NPA.

Environmental and ecological impacts

The observed warming and drought in the NPA have reduced water availability, altering hydrology (Pessacg et al. 2020; Hurtado et al. 2023). Over the past decades, river streamflow has shown negative trends annually (Masiokas et al. 2019) and in summer (Lauro et al. 2019) related to the observed decrease in annual precipitation, especially in rainy months (April to September). As NPA rivers depend on glaciers and snowmelt, rising summer temperatures and higher and positive temperature anomalies accelerate melting, while warmer winters reduce snow accumulation, driving glacier retreat. Glacier mass loss increased between 2010 and 2018 (Cordero et al. 2019; Masiokas et al. 2020) linked with the stepper increase in mean temperature from 2007, leading to a 50% rise in the glacial lake area (1986-2016) (Shugar et al. 2020). The increase in glacier retreat has led to catastrophic events associated with glacial lake formation, such as glacial lake outburst floods (GLOF), as well as continuous changes in physical and chemical variables in aquatic and terrestrial environments. Meltwater-induced changes in aquatic environments (Balseiro et al. 2022) have profoundly affected the physiology, metabolism and trophic interactions of streams (Martyniuk et al. 2014; Martyniuk et al. 2019; Martyniuk et al. 2022), and lake biota (Laspoumaderes et al. 2013; Bastidas Navarro et al. 2018; Modenutti et al. 2023).

The NPA hosts one of Earth's steepest plant productivity gradients, and fire activity is highly sensitive to weather conditions (Kitzberger et al. 2022). Projections indicate increased fire probabilities under warmer-drier conditions, with fire activity expected to rise throughout the 21st century (Veblen et al. 2011). Given fire sensitivity to climate variability (Holz et al. 2012; Holz et al. 2017) and ongoing warming and drying, areas receiving ~1000 mm/y of precipitation may see the highest fire occurrence (Kitzberger et al. 2022). As was observed here, precipitation declines in the NPA and isohyets retract westward, consequently, more areas may reach this threshold, increasing fire risk.

Acknowledgments. I thank two anonymous reviewers whose comments and suggestions significantly improved this manuscript. I thank all data providers: National Water Information System of the Secretary of Infrastructure and Water Policy of Argentina (SNIH), the Meteorological Information Center of the National Meteorological Service (SMN), and the Interjurisdictional Basin Authority of the Limay, Neuquen, and Negro Rivers (AIC).

Data availability. All the data generated and analyzed during the current study is available at the Universidad del Comahue's data repository: rdi.uncoma.edu.ar/handle/uncomaid/18107.

References

Arblaster, J. M., and G. A. Meehl. 2006. Contributions of External Forcings to Southern Annular Mode Trends. Journal of Climate 19:2896-2905. https://doi.org/10.1175/JCLI3774.1.

Arias, P. A., R. Garreaud, G. Poveda, J. C. Espinoza, J. Molina-Carpio, M. Masiokas, M. Viale, L. Scaff, and P. J. van Oevelen. 2021. Hydroclimate of the Andes Part II: Hydroclimate Variability and Sub-Continental Patterns. Frontiers in Earth Science 8. https://doi.org/10.3389/feart.2020.505467.

Balseiro, E., B. Modenutti, M. Bastidas Navarro, N. Martyniuk, L. Schenone, and C. Laspoumaderes. 2022. North Patagonian Andean Deep Lakes: Impact of Glacial Recession and Volcanic Eruption. Pp. 31-57 *in* Freshwaters and Wetlands of Patagonia. Springer Nature, Switzerland. https://doi.org/10.1007/978-3-031-10027-7_3.

Bastidas Navarro, M., N. Martyniuk, E. Balseiro, and B. Modenutti. 2018. Effect of glacial lake outburst floods on the light climate in an Andean Patagonian lake: implications for planktonic phototrophs. Hydrobiologia 816:39-48. https://doi.org/10.1007/s10750-016-3080-4.

Berman, A. L., G. Silvestri, and R. Compagnucci. 2012. Eastern Patagonia Seasonal Precipitation: Influence of Southern Hemisphere Circulation and Links with Subtropical South American Precipitation. Journal of Climate 25:6781-6795. https://doi.org/10.1175/jcli-d-11-00514.1.

Berri, G. J., E. Bianchi, and G. V. Müller. 2019. El Niño and La Niña influence on mean river flows of southern South America in the 20th century. Hydrological Sciences Journal 64:900-909. https://doi.org/10.1080/02626667.2019.1609681.

Campbell, I., and J. A. Renwick. 2023. Southern Hemisphere Storm Tracks and Large-Scale Variability: What Do the Latest Reanalyses Say? Journal of Climate 36:5549-5567. https://doi.org/10.1175/jcli-d-22-0726.1.

Cleveland, W. S., and E. Grosse. 1991. Computational methods for local regression. Statistics computing 1:47-62. https://doi.org/10.1007/BF01890836.

Condom, T., R. Martínez, J. D. Pabón, F. Costa, L. Pineda, J. J. Nieto, F. López, and M. Villacis. 2020. Climatological and hydrological observations for the South American Andes: in situ stations, satellite, and reanalysis data sets. Frontiers in Earth Science 8:92. https://doi.org/10.3389/feart.2020.00092.

Cordero, R. R., V. Asencio, S. Feron, A. Damiani, P. J. Llanillo, E. Sepulveda, J. Jorquera, J. Carrasco, and G. Casassa. 2019. Dry-Season Snow Cover Losses in the Andes (18 degrees-40 degrees S) driven by Changes in Large-Scale Climate Modes. Scientific Reports 9:16945. https://doi.org/10.1038/s41598-019-53486-7.

Falvey, M., and R. D. Garreaud. 2009. Regional cooling in a warming world: Recent temperature trends in the southeast Pacific and along the west coast of subtropical South America (1979-2006). Journal of Geophysical Research 114. https://doi.org/10.1029/2008jd010519.

Fernandez, E., C. Whitney, and E. Luedeling. 2020. The importance of chill model selection — a multi-site analysis. European Journal of Agronomy 119:126103.

Fogt, R. L., and G. J. Marshall. 2020. The Southern Annular Mode: Variability, trends, and climate impacts across the Southern Hemisphere. WIREs Climate Change 11. https://doi.org/10.1002/wcc.652.

Garreaud, R. 2009. The Andes climate and weather. Advances in Geosciences 22:3-11. https://doi.org/10.5194/adgeo-22-3-2009.

Garreaud, R. 2018. Record-breaking climate anomalies lead to severe drought and environmental disruption in western Patagonia in 2016. Climate Research 74:217-229. https://doi.org/10.3354/cr01505.

Giorgi, F., F. Raffaele, and E. Coppola. 2019. The response of precipitation characteristics to global warming from climate projections. Earth System Dynamics 10:73-89. https://doi.org/10.5194/esd-10-73-2019.

González, M. 2015. Statistical Seasonal Rainfall Forecast in the Neuquén River Basin (Comahue Region, Argentina). Climate 3:349-364. https://doi.org/10.3390/cli3020349.

González, M., E. M. Garbarini, and P. E. Romero. 2015. Rainfall patterns and the relation to atmospheric circulation in northern Patagonia (Argentina). Marine Environmental Research 41:85-100.

González, M. H., A. L. Rolla, and M. V. Sanchez. 2022. Seasonal probabilistic precipitation prediction in Comahue region (Argentina) using statistical techniques. Theoretical and Applied Climatology 151:1483-1495. https://doi.org/10.1007/s00704-022-04324-w.

González, M. H., and C. S. Vera. 2010. On the interannual wintertime rainfall variability in the Southern Andes. International Journal of Climatology 30:643-657. https://doi.org/10.1002/joc.1910.

Guisan, A., T. C. J. Edwards, and T. Hastie. 2002. Generalized linear and generalized additive models in studies of species distributions: setting the scene. Ecological Modelling 157:89-100. https://doi.org/10.1016/S0304-3800(02)00204-1.

Guttman, N. B. 1999. Accepting the standardized precipitation index: a calculation algorithm. JAWRA Journal of the American Water Resources Association 35:311-322. https://doi.org/10.1111/j.1752-1688.1999.tb03592.x.

Holz, A., T. Kitzberger, J. Paritsis, and T. T. Veblen. 2012. Ecological and climatic controls of modern wildfire activity patterns across southwestern South America. Ecosphere 3:1-25. https://doi.org/10.1890/ES12-00234.1.

Holz, A., J. Paritsis, I. A. Mundo, T. T. Veblen, T. Kitzberger, G. J. Williamson, E. Aráoz, C. Bustos-Schindler, M. E. González, and H. R. Grau. 2017. Southern Annular Mode drives multicentury wildfire activity in southern South America. Proceedings of the National Academy of Sciences 114:9552-9557. https://doi.org/10.1073/pnas.1705168114.

Hurtado, S. I., M. Calianno, S. Adduca, and M. H. Easdale. 2023. Drylands becoming drier: evidence from North Patagonia, Argentina. Regional Environmental Change 23:1-12. https://doi.org/10.1007/s10113-023-02160-w.

Huss, M., B. Bookhagen, C. Huggel, D. Jacobsen, R. Bradley, J. Clague, M. Vuille, W. Buytaert, D. Cayan, G. Greenwood, B. Mark, A. Milner, R. Weingartner, and M. S. Winder. 2017. Towards mountains without permanent snow and ice.

Earth's Future 5:418-435. https://doi.org/10.1002/2016EF000514.

IPCC. 2014. Climate Change 2014: Synthesis Report. Contribution of Working Groups I, II and III to the Fifth Assessment Report of the Intergovernmental Panel on Climate Change. IPCC, Cambridge, United Kingdom and New York, NY, USA.

IPCC. 2021. Climate Change 2021: The Physical Science Basis. Contribution of Working Group I to the Sixth Assessment Report of the Intergovernmental Panel on Climate Change. Cambridge University Press, Cambridge, United Kingdom and New York, NY, USA.

Jobbágy, E., J. M. Paruelo, and R. León. 1995. Estimación del régimen de precipitación a partir de la distancia a la cordillera en el noroeste de la Patagonia. Ecologia Austral 5:47-53.

Kitzberger, T., F. Tiribelli, I. Barberá, J. H. Gowda, J. M. Morales, L. Zalazar, and J. Paritsis. 2022. Projections of fire probability and ecosystem vulnerability under 21st century climate across a trans-Andean productivity gradient in Patagonia. Science of the total environment 839:156303. https://doi.org/10.1016/j.scitotenv.2022.156303.

Kleijnen, J. P. 2017. Kriging: methods and applications. CentER Discussion Paper Series No. 2017-047. https://doi.org/10.2139/ssrn.3075151.

Laspoumaderes, C., B. Modenutti, M. S. Souza, M. Bastidas Navarro, F. Cuassolo, and E. Balseiro. 2013. Glacier melting and stoichiometric implications for lake community structure: zooplankton species distributions across a natural light gradient. Global Change Biology 19:316-326. https://doi.org/10.1111/gcb.12040.

Lauro, C., A. I. Vich, and S. M. Moreiras. 2019. Streamflow variability and its relationship with climate indices in western rivers of Argentina. Hydrological Sciences Journal 64:607-619. https://doi.org/10.1080/02626667.2019.1594820.

Lindsey, R., and L. Dahlman. 2020. Monthly Global Climate Report for Annual 2021: Climate change: Global temperature. NOAA National Centers for Environmental Information 16.

Luedeling, E. 2018. Interpolating hourly temperatures for computing agroclimatic metrics. International Journal of Biometeorology 62:1799-1807. https://doi.org/10.1007/s00484-018-1582-7.

Marcott, S. A., J. D. Shakun, P. U. Clark, and A. C. Mix. 2013. A reconstruction of regional and global temperature for the past 11300 years. Science 339:1198-1201. https://doi.org/10.1126/science.1228026.

Martyniuk, N., B. Modenutti, and E. Balseiro. 2014. Can increased glacial melting resulting from global change provide attached algae with transient protection against high irradiance? Freshwater Biology 59:2290-2302. https://doi.org/10.1111/fwb.12431.

Martyniuk, N., B. Modenutti, and E. G. Balseiro. 2019. Seasonal variability in glacial influence affects macroinvertebrate assemblages in North-Andean Patagonian glacier-fed streams. Inland Waters 9:522-533. https://doi.org/10.1080/20442041.2019.1624115.

Martyniuk, N., M. S. Souza, M. Bastidas Navarro, E. Balseiro, and B. Modenutti. 2022. Nutrient limitation affects biofilm enzymatic activities in a glacier-fed river. Hydrobiologia 849:2877-2894. https://doi.org/10.1007/s10750-022-04857-1.

Masiokas, M. H., L. Cara, R. Villalba, P. Pitte, B. H. Luckman, E. Toum, D. A. Christie, C. Le Quesne, and S. Mauget. 2019. Streamflow variations across the Andes (18 degrees-55 degrees S) during the instrumental era. Scientific Reports 9:17879. https://doi.org/10.1038/s41598-019-53981-x.

Masiokas, M. H., A. Rabatel, A. Rivera, L. Ruiz, P. Pitte, J. L. Ceballos, G. Barcaza, A. Soruco, F. Bown, E. Berthier, I. Dussaillant, and S. MacDonell. 2020. A Review of the Current State and Recent Changes of the Andean Cryosphere. Frontiers in Earth Science 8. https://doi.org/10.3389/feart.2020.00099.

McKee, T. B., N. J. Doesken, and J. Kleist. 1993. The relationship of drought frequency and duration to time scales. Pp. 179-183 *in* Proceedings of the 8th Conference on Applied Climatology. Boston.

Messager, M. L., B. Lehner, G. Grill, I. Nedeva, and O. Schmitt. 2016. Estimating the volume and age of water stored in global lakes using a geo-statistical approach. Nature Communications 7:13603. https://doi.org/10.1038/ncomms13603.

Modenutti, B., N. Martyniuk, M. Bastidas Navarro, and E. Balseiro. 2023. Glacial Influence Affects Modularity in Bacterial Community Structure in Three Deep Andean North-Patagonian Lakes. Microbial Ecology 86:1869-1880. https://doi.org/10.1007/s00248-023-02184-z.

Morales, M. S., E. R. Cook, J. Barichivich, D. A. Christie, R. Villalba, C. LeQuesne, A. M. Srur, M. E. Ferrero, et al. 2020. Six hundred years of South American tree rings reveal an increase in severe hydroclimatic events since mid-20th century. Proceedings of the National Academy of Sciences of the United States of America 117:16816-16823. https://doi.org/10.1073/pnas.2002411117.

National Drought Mitigation Center, C. 2018. SPI Generator [software]. University of Nebraska-Lincoln.

Olmo, M., M. L. Bettolli, and M. Rusticucci. 2020. Atmospheric circulation influence on temperature and precipitation individual and compound daily extreme events: Spatial variability and trends over southern South America. Weather and Climate Extremes 29. https://doi.org/10.1016/j.wace.2020.100267.

Paruelo, J. M., A. Beltran, E. Jobbágy, O. Sala, and R. Golluscio. 1998. The climate of Patagonia: general patterns and controls on biotic processes. Ecología Austral 8:85-101.

Pessacg, N., S. Flaherty, S. Solman, and M. Pascual. 2020. Climate change in northern Patagonia: critical decrease in water resources. Theoretical and Applied Climatology 140:807-822. https://doi.org/10.1007/s00704-020-03104-8.

R Core Team. 2020. A language and environment for statistical computing. R Foundation for Statistical Computing, Vienna, Austria.

Rivera, J., and O. Penalba. 2014. Trends and Spatial Patterns of Drought Affected Area in Southern South America. Climate 2:264-278. https://doi.org/10.3390/cli2040264.

Rusticucci, M., and M. Barrucand. 2004. Observed Trends and Changes in Temperature Extremes over Argentina. Journal of Climate 17:4099-4107. https://doi.org/10.1175/1520-0442(2004)017%3C4099:OTACIT%3E2.0.CO;2.

Shugar, D. H., A. Burr, U. K. Haritashya, J. S. Kargel, C. S. Watson, M. C. Kennedy, A. R. Bevington, R. A. Betts, S. Harrison, and K. Strattman. 2020. Rapid worldwide growth of glacial lakes since 1990. Nature Climate Change 10: 939-945. https://doi.org/10.1038/s41558-020-0855-4.

Silvestri, G., and C. Vera. 2009. Nonstationary impacts of the southern annular mode on Southern Hemisphere climate. Journal of Climate 22:6142-6148. https://doi.org/10.1175/2009JCLI3036.1.

Veblen, T. T., A. Holz, J. Paritsis, E. Raffaele, T. Kitzberger, and M. Blackhall. 2011. Adapting to global environmental change in Patagonia: what role for disturbance ecology? Austral Ecology 36:891-903. https://doi.org/10.1111/j.1442-9993.2010.02236.x.

Vuille, M., E. Franquist, R. Garreaud, W. S. Lavado Casimiro, and B. Cáceres. 2015. Impact of the global warming hiatus on Andean temperature. Journal of Geophysical Research: Atmospheres 120:3745-3757. https://doi.org/10.1002/2015jd023126.

WMO. 2021. State of the Climate in Latin America and the Caribbean. World Meteorological Organization, Strategic Communications Office, Geneva, Switzerland.

Wood, S. N. 2008. Fast stable direct fitting and smoothness selection for generalized additive models. The Journal of the Royal Statistical Society, Series B 70:495-518. https://doi.org/10.1111/j.1467-9868.2007.00646.x.